

Unveiling the Double Triplet Nature of the 2Ag State in Conjugated Stilbenoid Compounds to Achieve Efficient Singlet Fission

Letizia Mencaroni,^a Martina Alebardi,^a Fausto Elisei,^a Irena Škorić,^b Anna Spalletti,^a Benedetta Carlotti*,^a

^a Department of Chemistry, Biology and Biotechnology, University of Perugia, via elce di sotto 8, 06123 Perugia, Italy.

^b Department of Organic Chemistry, Faculty of Chemical Engineering and Technology, University of Zagreb, 10000 Zagreb, Croatia.

ELECTRONIC SUPPORTING INFORMATION

Table of contents

1. Experimental section
2. Spectral and fluorescence properties
3. Triplet properties
4. Ultrafast spectroscopy
5. Phosphorescence measurements
6. Quantum mechanical calculations

1. Experimental section

Materials and methods

Chemicals. The investigated compounds were synthesized according to the procedures described in previous papers.^{1–4} Spectral and photophysical properties were recorded in many solvents with spectroscopic grade: Perfluorohexane (PFHx, Sigma-Aldrich), 2-Methylbutane (IP, Sigma-Aldrich), Hexane (Hx, Sigma-Aldrich), 3-Methylpentane (3-MP, Sigma-Aldrich), methylcyclohexane (MeCH, Sigma-Aldrich), Decahydronaphthalene (DHN, Sigma-Aldrich), Toluene (Tol, Sigma-Aldrich), Anisole (An, Sigma-Aldrich), Dimethylsulfoxide (DMSO, Carlo Erba), Bromonaphthalene (BrN, Sigma-Aldrich) and Diiodomethane (DIM, Sigma.Aldrich).

Photophysical characterization. Stationary absorption measurements were carried out by a Varian Cary 1 UV-Visible spectrophotometer. A FluoroMax-4P spectrofluorimeter by HORIBA scientific operated by FluorEssence and a FS5 Spectrofluorimeter by Edinburgh Instruments operated by Fluoracle software were used instead for excitation and emission fluorescence spectra at room temperature. Air-equilibrated dilute solutions (absorbance < 0.1 at the excitation wavelength) were used for the fluorimetric measurements. The fluorescence quantum yields (Φ_F , experimental error $\pm 10\%$ and 20% when $\Phi_F \leq 10^{-4}$) were obtained by employing tetracene ($\Phi_F = 0.17$ in air-equilibrate cyclohexane) and 9,10-diphenylanthracene ($\Phi_F = 0.73$ in air-equilibrated cyclohexane) as reference compounds,⁵ taking also into account the different refractive indexes of the used solvents.

Triplet properties were measured by laser flash photolysis (Edinburgh LP980) at 355 nm (third harmonic of a Continuum Surelite II Nd:YAG laser, Spectra Physics) with nanosecond time-resolution (pulse width 7 ns and laser energy < 1 mJ per pulse) coupled with a PMT for signal detection. The excitation at 355 nm was the pump-pulse while a pulsed xenon lamp was used to probe the absorption properties of the produced excited states. The experimental setup was calibrated by an optical matched solution of benzophenone (Bz) in MeCN ($\Phi_T = 1$ and $\epsilon_T = 6500 \text{ M}^{-1} \text{ cm}^{-1}$ at 520 nm).⁶ Triplet–triplet absorption coefficients (ϵ_T) were retrieved from previous investigations.^{4,7,8} The triplet quantum yields, Φ_T , were determined (estimated uncertainty of $\pm 15\%$) by an

actinometry approach considering Bz or thioxanten-9-one (TX) in AcCN ($\Phi_T = 0.66^9$ and $\varepsilon_T = 30000 \text{ M}^{-1} \text{ cm}^{-1}$ at $\lambda_T = 630 \text{ nm}$)¹⁰ and anthracene (A) in CH ($\Phi_T = 0.71$ and $\varepsilon_T = 45500 \text{ M}^{-1} \text{ cm}^{-1}$ at $\lambda_T = 422 \text{ nm}$)⁶ as references. All measurements were performed by purging the sample with pure molecular nitrogen. The study of the concentration effect on Φ_T was intrinsically limited by the experimental technique itself. Therefore, a narrow range of concentrations (corresponding to absorbances: $A_{355} \approx 0.1, 0.5$ up to $A_{355} = 1$) could be analyzed. The detailed methodologies concerning the determination of the triplet extinction coefficient and the quantum yield, jointly to its concentration dependence, have been extensively discussed in the Supporting Information of Ref¹¹.

The experimental setup for ultrafast transient absorption experiments have been previously reported.^{12–15} The 400 nm excitation pulses (ca. 60 fs) were generated by an amplified Ti:Sapphire laser system (Spectra Physics). The Helios transient absorption spectrometer (Ultrafast Systems) is characterized by a temporal resolution of about 150 fs and a spectral resolution of 1.5 nm. A small portion of the 800-nm light passes through an optical delay line (time window of 3200 ps) and is focused onto a Sapphire crystal (2 mm thick) to generate a white-light in the 450–800 nm spectral range (probe pulse). All measurements were carried out under the magic angle in 2 mm cell at an absorbance of about 0.5 at 400 nm (concentration $\approx 2 \times 10^{-4} \text{ M}$). The solution was stirred during the experiments to avoid photoproduct interferences. Photodegradation was checked recording the absorption spectra before and after the time-resolved measurements, where no significant change was observed. The experimental 3D data matrices were firstly analyzed performing the Global Analysis by Surface Xplorer PRO (Ultrafast Systems) software, and successively through GloTarAn software in order to obtain the Evolution-Associated Spectra (EAS) considering a consecutive kinetic model. The statistical uncertainties on the transient lifetimes provided by the fitting were found to be ca. 10%.

Quantum mechanical calculations. Quantum mechanical calculations were performed by using the Gaussian 16 package.¹⁶ DFT with the CAM–B3LYP functional was chosen as the method to optimize the ground state geometry of these small organic push-pull systems and to derive their properties.¹⁷ In contrast the lowest singlet excited states were investigated using TD–DFT excited-state calculations with the CAM–B3LYP functional. Every calculation was submitted using 6–31+G(d,p) as the basis set including the solvent effect (CH) according to the conductor-like polarizable continuum model (CPCM).¹⁸

2. Spectral and fluorescence properties

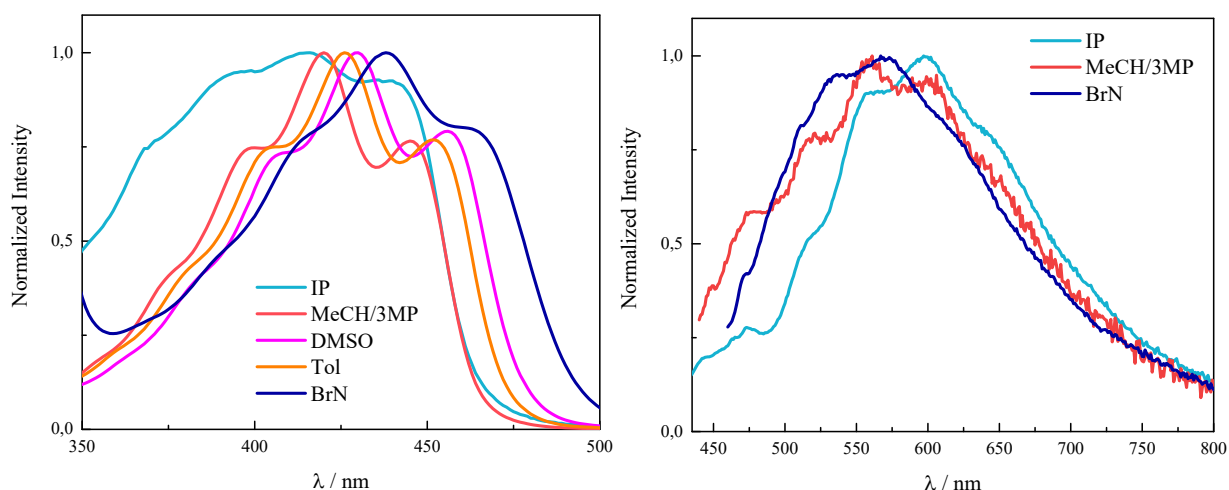


Figure ESI.1. Normalized absorption (left) and emission (right) spectra of 2,5-(PhBu)₂T in solvents of different polarizability.

Table ESI.1. Spectral and fluorescence properties of **2,5-(PhBu)₂T** in solvents of different polarizability. The main absorption/emission maximum is in bold; sh means shoulder.

2,5-(PhBu)₂T	n	ϵ	$\lambda_{\text{abs}} / \text{nm}$	$\lambda_{\text{em}} / \text{nm}$
IP	1.3540	1.8275	369 ^{sh} 392 415 440	474 ^{sh} 514 ^{sh} 557 598 647 ^{sh}
MeCH-3MP (9/1)	1.3812	2.0075	373 ^{sh} 398 420 445	474 ^{sh} 516 561 598 649 ^{sh}
DMSO	1.4793	46.68	381 ^{sh} 406 430 456	
Tol	1.49693	2.379	379 ^{sh} 404 426 451	
BrN	1.6570	4.768	387 ^{sh} 413 438 465	472 ^{sh} 510 ^{sh} 534 567 619 ^{sh}

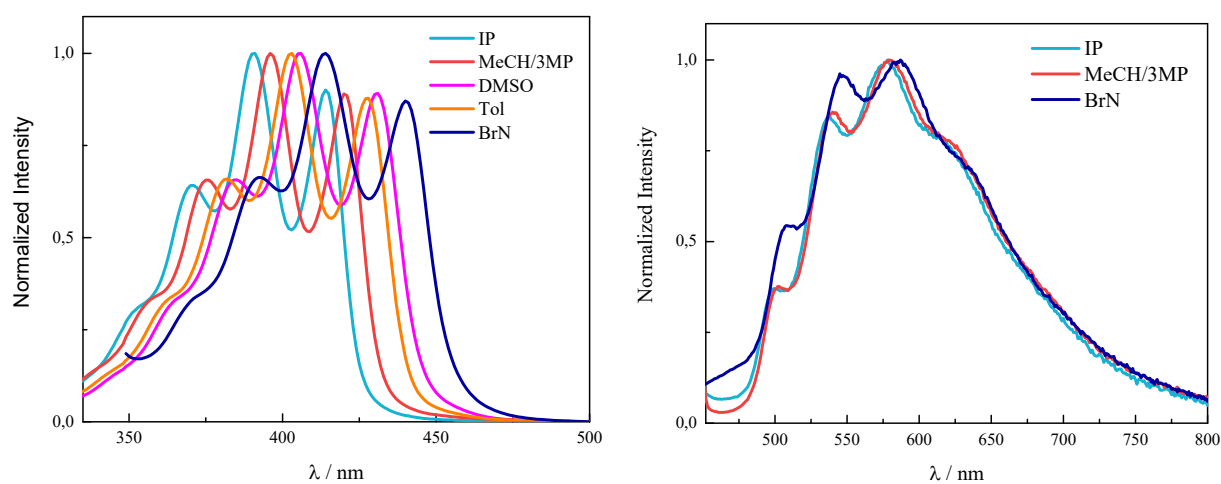


Figure ESI.2. Normalized absorption (left) and emission (right) spectra of **D2TO** in solvents of different polarizability.

Table ESI.2. Spectral and fluorescence properties of **D2TO** in solvents of different polarizability. The main absorption/emission maximum is in bold; sh means shoulder.

D2TO	n	ϵ	$\lambda_{\text{abs}} / \text{nm}$	$\lambda_{\text{em}} / \text{nm}$
IP	1.3540	1.8275	350 ^{sh} 370 391 414	498 ^{sh} 536 577 623 ^{sh}
MeCH-3MP (9/1)	1.3812	2.0075	356 ^{sh} 376 396 420	502 ^{sh} 541 579 625 ^{sh}
DMSO	1.4793	46.68	363 ^{sh} 385 405 431	
Tol	1.49693	2.379	361 ^{sh} 382 403 427	
BrN	1.6570	4.768	370 ^{sh} 392 414 440	508 ^{sh} 548 587 635 ^{sh}

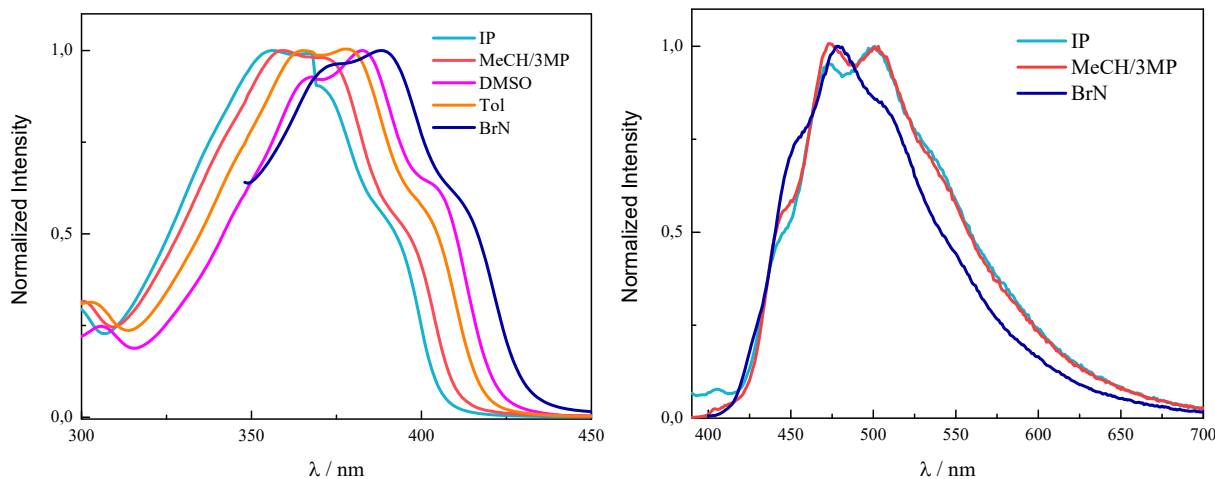


Figure ESI.3. Normalized absorption (left) and emission (right) spectra of **1NPH** in solvents of different polarizability.

Table ESI.3. Spectral and fluorescence properties of **1NPH** in solvents of different polarizability. The main absorption/emission maximum is in bold; sh means shoulder.

1NPH	n	ϵ	$\lambda_{\text{abs}} / \text{nm}$	$\lambda_{\text{em}} / \text{nm}$
IP	1.3540	1.8275	356 371 392^{sh}	444 ^{sh} 473 501 539 ^{sh}
MeCH-3MP (9/1)	1.3812	2.0075	359 371 396^{sh}	445 ^{sh} 472 501 538 ^{sh}
DMSO	1.4793	46.68	367 383 404 ^{sh}	
Tol	1.49693	2.379	366 378 401^{sh}	
BrN	1.6570	4.768	373 388 413^{sh}	450 ^{sh} 480 508 ^{sh} 550 ^{sh}

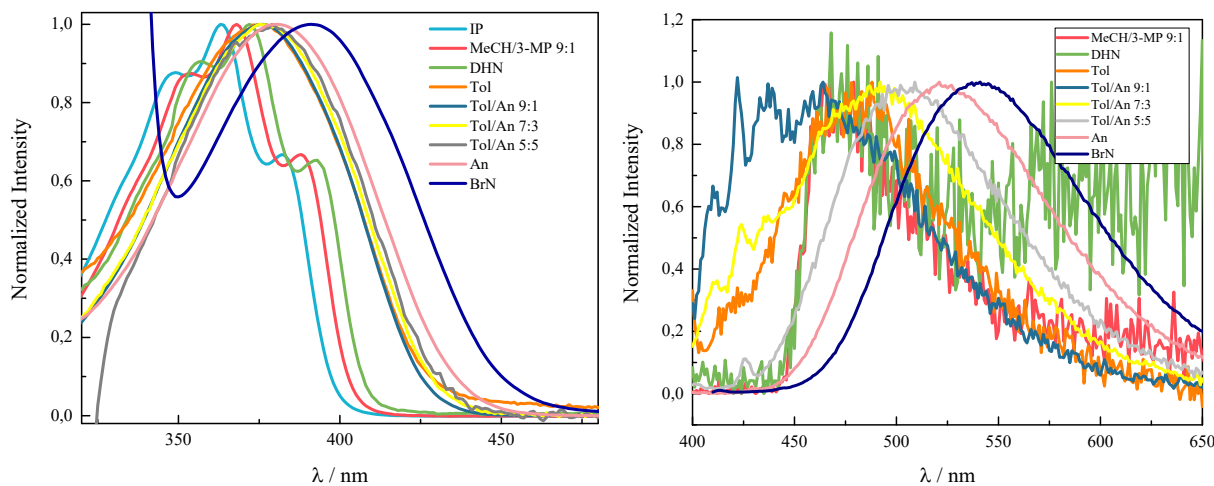


Figure ESI.4. Normalized absorption (left) and emission (right) spectra of **DF** in solvents of different polarizability.

Table ESI.4. Spectral and fluorescence properties of **DF** in solvents of different polarizability. The main absorption/emission maximum is in bold.

DF	n	ϵ	$\lambda_{\text{abs}} / \text{nm}$	$\lambda_{\text{em}} / \text{nm}$
IP	1.3540	1.8275	349 363 383	
MeCH-3MP (9/1)	1.3812	2.008	353 368 389	479
DHN	1.4758	2.154	357 372 393	468
Tol	1.49693	2.379	375	488
Tol/An 9:1	1.4989	2.574	376	464
Tol/An 7:3	1.5031	2.964	377	492
Tol/An 5:5	1.5073	3.355	379	509
An	1.5179	4.330	382	521
BrN	1.6570	4.768	390	541

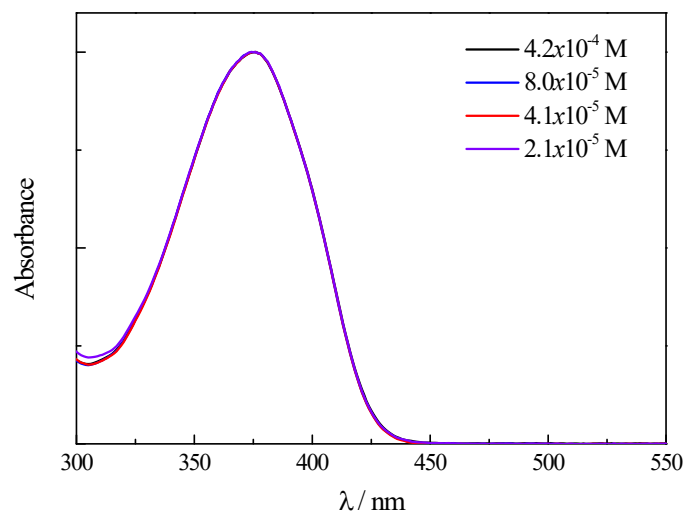


Figure ESI.5. Absorption spectra of compound **DF** in Tol as a function of concentration.

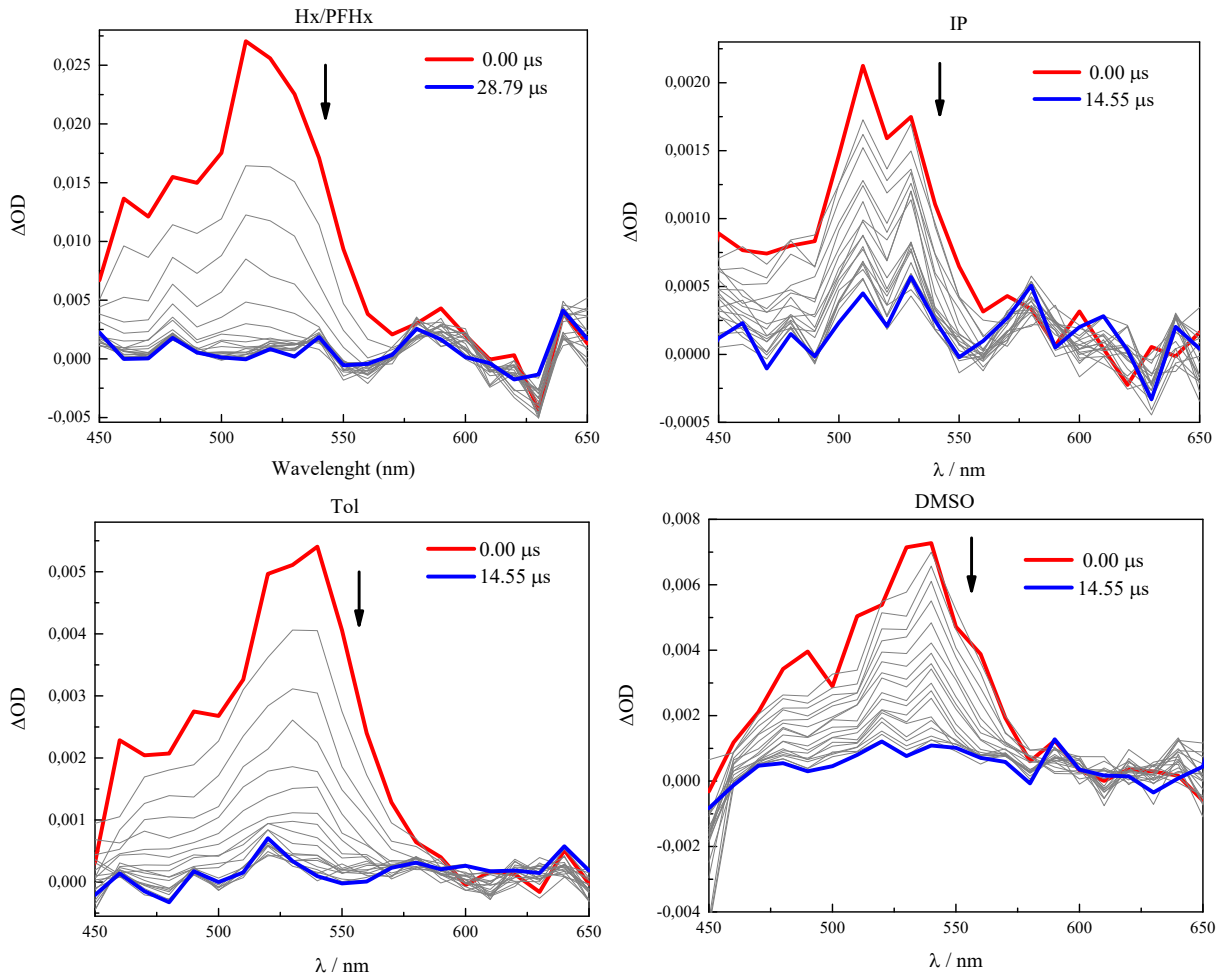
Table ESI.5. Fluorescence properties of **2,5-(PhBu)₂T** and **D2TO** in solvents of different polarizability.

Sample	Solvent	n	Φ_F	τ_F / ns	k_F / s^{-1}
2,5-(PhBu)₂T	IP	1.3540	0.0006	0.305	2.0×10^6
	MeCH/3-MP 9:1	1.3812	0.0012 ^a	0.290 ^a	4.1×10^6
	DMSO	1.4793	0.0021	0.510	4.1×10^6
	Tol	1.49693	0.0028	0.295 ^b	9.5×10^6
	BrN	1.6570	0.0046	0.650	7.1×10^6
D2TO	MeCH/3-MP 9:1	1.3812	0.003	0.958	3.1×10^6
	Tol	1.49693	0.007	1.07	6.5×10^6

^aFrom ref. 2

^bFrom Femtosecond Transient Absorption measurements

3. Triplet properties



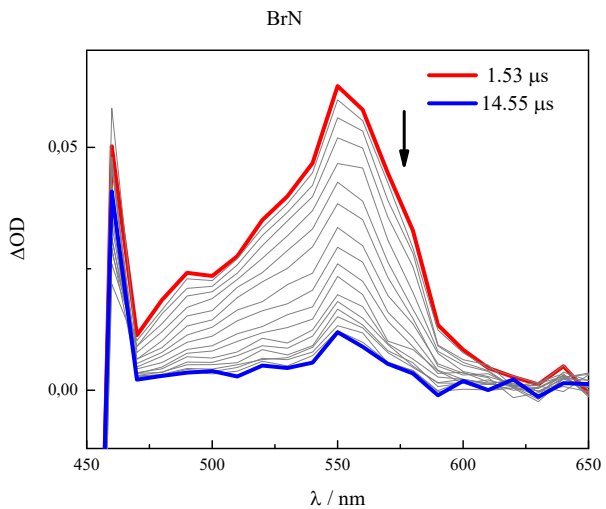


Figure ESI.6. Triplet transient absorption spectra obtained in N₂-purged solutions of **2,5-(2TE)₂T** in solvents of different polarizability.

Table ESI.6. Triplet properties of **2,5-(2TE)₂T** in solvents of different polarizability.

Solvent	Φ_T (N ₂)	λ_T / nm	τ_T (air) / μ s	τ_T (N ₂) / μ s	k_T / 10^7 s ⁻¹
Hx/PFHx	0.09	520	0.074	5.60	4.3
IP	0.09	510	0.478	7.03	5.0
DMSO	0.18	545	0.590	8.10	9.5
Tol	0.14	540	0.019	6.29	7.8
BrN	0.19	550	0.890	7.03	12.7

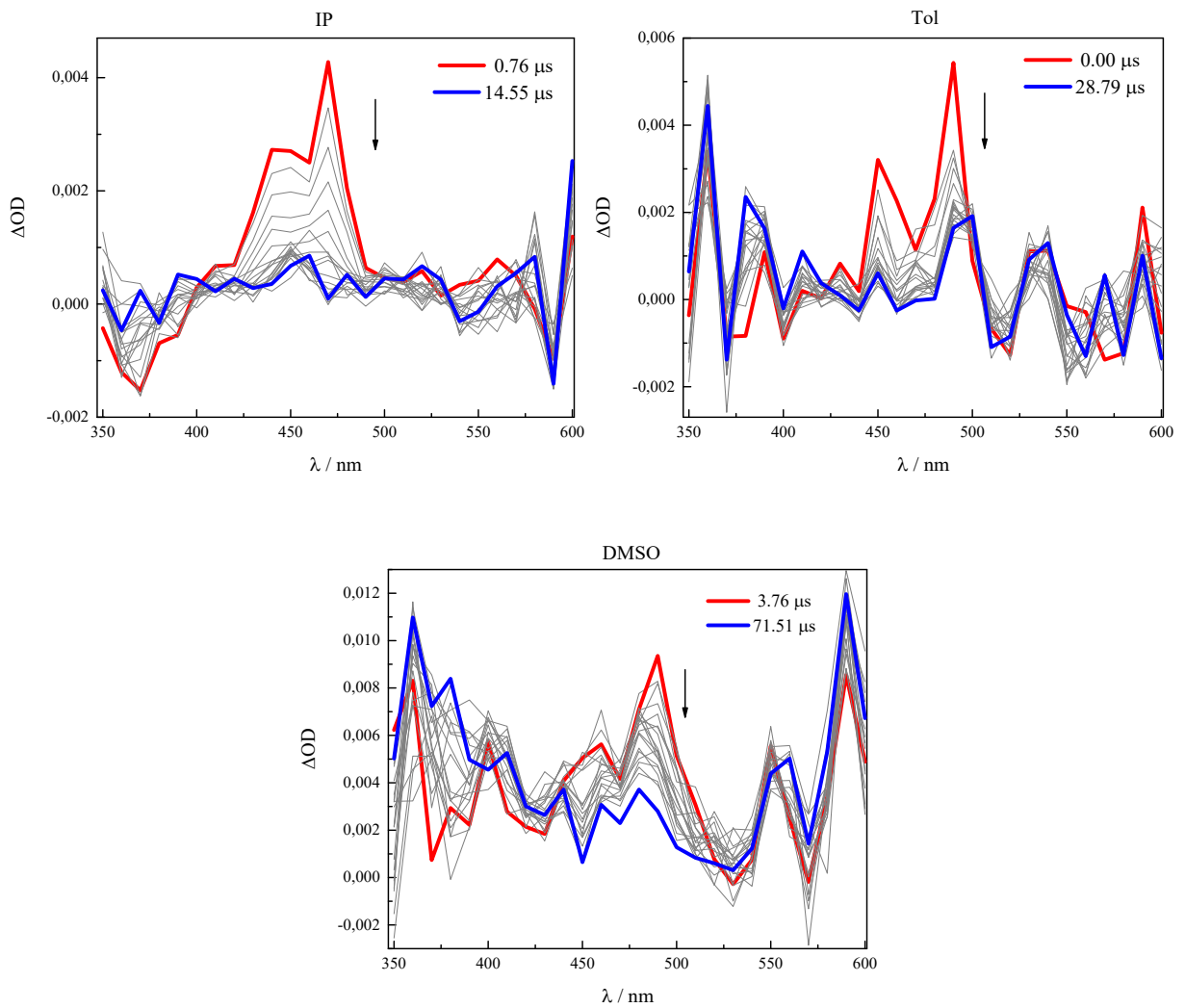


Figure ESI.7. Triplet transient absorption spectra obtained in N_2 -purged solutions of **1NPH** in IP, Tol and DMSO.

Table ESI.7. Triplet properties of **1NPH** in solvents of different polarizability.

Solvent	$\Phi_T (N_2)$	λ_T / nm	$\tau_T (N_2) / \mu s$	$k_T / 10^7 \text{ s}^{-1}$
IP	0.01	470	1.68	0.088
DMSO	0.01	490	18.9	0.087
Tol	0.02	490	14.5	0.204

4. Ultrafast Spectroscopy

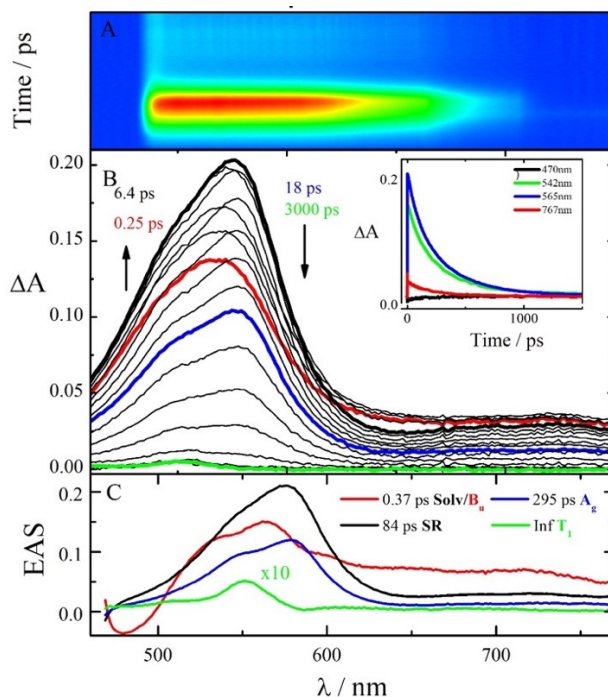


Figure ESI.8. Femtosecond Transient Absorption measurements of compound **2,5-(PhBu)₂T** in Tol: experimental 3D data matrix (panel A); main time-resolved absorption spectra (panel B) and representative kinetics recorded at significant wavelengths (inset); Evolution Associated Spectra (EAS) obtained by Global Analysis.

Table ESI.8. Femtosecond transient absorption and fluorescence up conversion measurements of compound **2,5-(PhBu)₂T** in solvents of different polarizability.

Solvent	τ_{TA} / ps	τ_{FUC} / ps	Assignment
IP	0.63	0.31	Solv./B _u
	55	30	SR
	280	305	A _g
	Inf		T ₁
MeCH/3-MP	0.30	0.35	Solv./B _u
	67	67	SR
	260	240	A _g
	Inf		T ₁
DMSO	0.52	0.64	Solv./B _u
	8.2	8.8	SR
	290	250	A _g
	Inf		T ₁
Tol	0.37	0.32	Solv./B _u
	84	9.0	VC
	295	82	A _g
	Inf		T ₁

BrN	0.84 70 315 Inf	0.96 25 400	Solv./ B_u SR A_g T_1
-----	--------------------------	-------------------	--------------------------------------

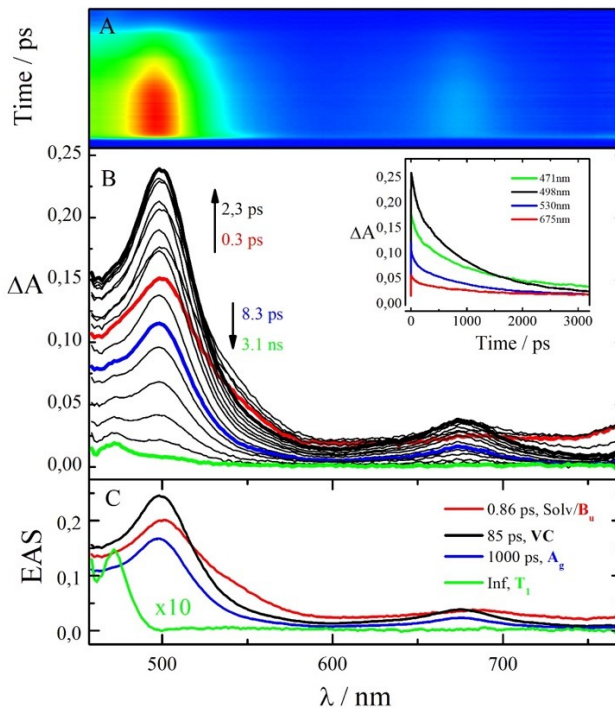


Figure ESI.9. Femtosecond Transient Absorption measurements of compound **D2TO** in Tol: experimental 3D data matrix (panel A); main time-resolved absorption spectra (panel B) and representative kinetics recorded at significant wavelengths (inset); Evolution Associated Spectra (EAS) obtained by Global Analysis.

Table ESI.9. Femtosecond transient absorption and fluorescence up conversion measurements of compound **D2TO** in solvents of different polarizability.

Solvent	τ_{TA} / ps	τ_{FUC} / ps	Assignment
IP	0.75		Solv./ B_u
	45		VC
	955		A_g
MeCH/3MP	0.36	0.28	Solv./ B_u
	74	74	VC
	900	1000	A_g
DMSO	0.63	0.32	Solv./ B_u
	270	205	VC
	1140	1000	A_g
Tol	0.86	0.32	Solv./ B_u
	85	90	VC
	1000	840	A_g
	Inf		T_1
BrN	0.78	0.46	Solv./ B_u

	115 1000 Inf	72 690	VC A_g T_1
--	--------------------	-----------	----------------------

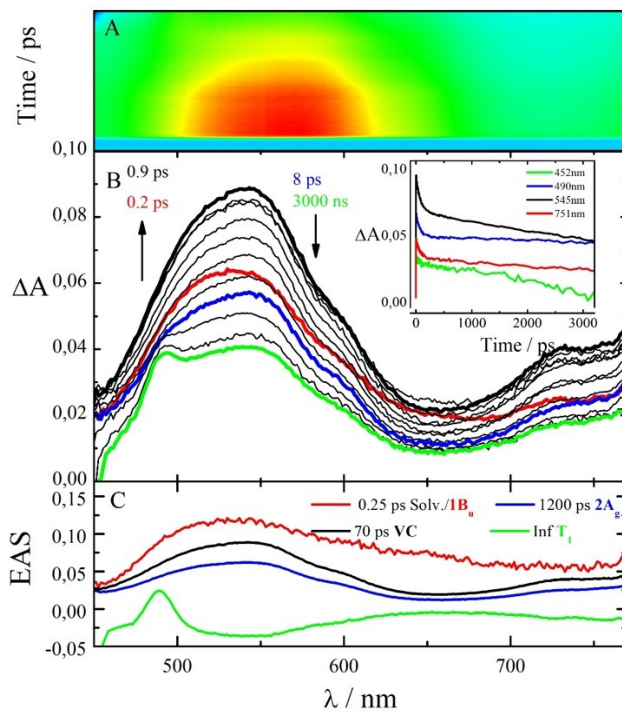


Figure ESI.10. Femtosecond Transient Absorption measurements of compound **1NPH** in Tol: experimental 3D data matrix (panel A); main time-resolved absorption spectra (panel B) and representative kinetics recorded at significant wavelengths (inset); Evolution Associated Spectra (EAS) obtained by Global Analysis.

Table ESI.10. Femtosecond transient absorption and fluorescence up conversion measurements of compound **1NPH** in solvents of different polarizability.

Solvent	τ_{TA} / ps	τ_{FUC} / ps	Assignment
IP	0.32	0.48	Solv./ B_u
	33	32	VC
	9400	9400	A_g
	Inf		T_1
MeCH/3MP	0.21	1.8	Solv./ B_u
	67	71	VC
	11000	6700	A_g
	Inf		T_1
DMSO	0.67		Solv./ B_u
	255		VC
	11500		A_g
	Inf		T_1
Tol	0.25		Solv./ B_u
	70		VC

	12000 Inf		A_g T_1
BrN	0.64 205 12000 Inf	0.64 440 12000	Solv./ B_u VC A_g T_1

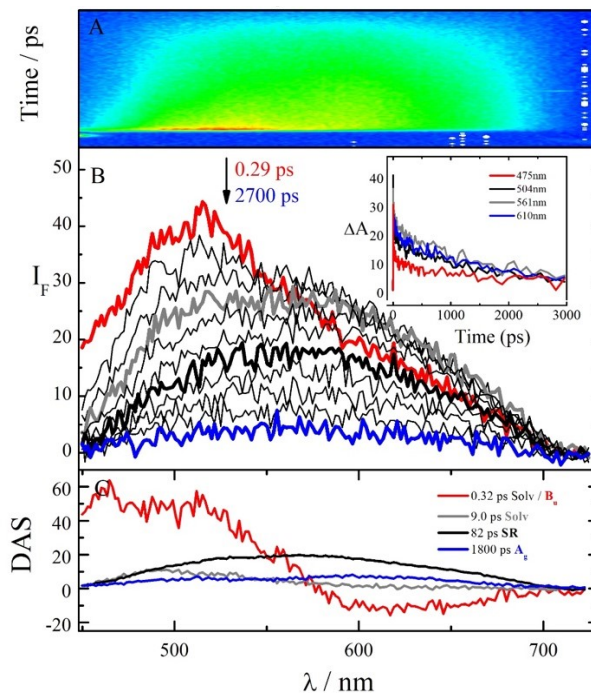


Figure ESI.11. Femtosecond Fluorescence Up-Conversion measurements of compound **2,5-(2TE)₂T** in Tol: experimental 3D data matrix (panel A); main time-resolved absorption spectra (panel B) and representative kinetics recorded at significant wavelengths (inset); Decay Associated Spectra (DAS) obtained by Global Analysis.

Table ESI.11. Femtosecond transient absorption and fluorescence up conversion measurements of compound **2,5-(2TE)₂T** in solvents of different polarizability.

Solvent	τ_{TA} / ps	τ_{FUC} / ps	Assignment
Hx/PFHx	0.44	0.58	Solv./B _u
	42	34	SR
	2100	2100	A _g
	Inf		T ₁
IP	0.93	0.50	Solv./B _u
	29	25	SR
	1400	1100	A _g
	Inf		T ₁
DMSO	0.64	0.64	Solv./B _u
	10	8.8	Solv.
	140	250	SR
	1900	1900	A _g
	Inf		T ₁
Tol	0.24	0.32	Solv. / B _u
	6.9	9.0	Solv.
	72	82	SR
	1800	1800	A _g
	Inf		T ₁
BrN	0.76	0.45	Solv.
	6.0	6.3	Solv.
	120	240	SR
	1500	1500	A _g
	Inf		T ₁

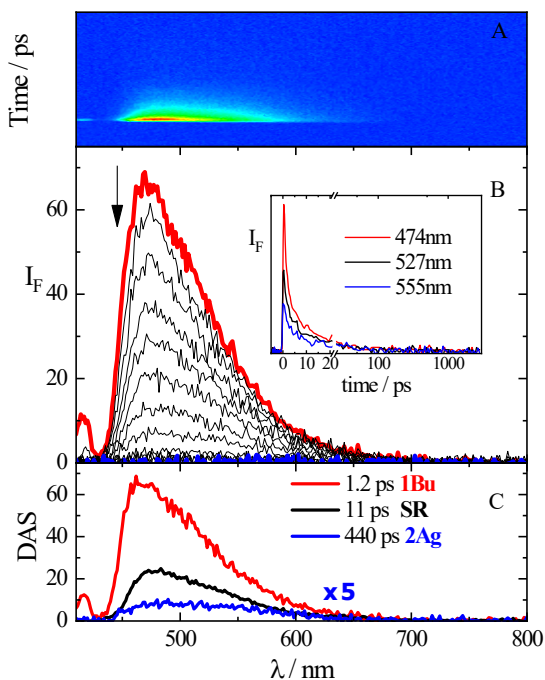


Figure ESI.12. Femtosecond Fluorescence Up-Conversion measurements of compound **PN** in Tol: experimental 3D data matrix (panel A); main time-resolved absorption spectra (panel B) and representative kinetics recorded at significant wavelengths (inset); Decay Associated Spectra (DAS) obtained by Global Analysis.

Table ESI.12. Femtosecond transient absorption and fluorescence up conversion measurements of compound **PN** in solvents of different polarizability.

Solvent	τ_{TA} / ps	Assignment
Tol	0.36 1.3 12 365 Inf	Solv./B _u Solv. SR A _g T ₁
Tol/An 7:3	0.66 14 380 Inf	Solv./B _u SR A _g T ₁
Tol/An 1:1	0.54 5.7 85 400 Inf	Solv./B _u SR ICT A _g T ₁
Tol/An 3:7	1.0 10 200 Inf	Solv./B _u SR ICT T ₁
An ^a	1.8 8.7 360 Inf	Solv./B _u SR ICT T ₁
DMSO	0.60 4.2 92 1500	Solv./B _u Solv. SR ICT

^a from ref.¹⁹

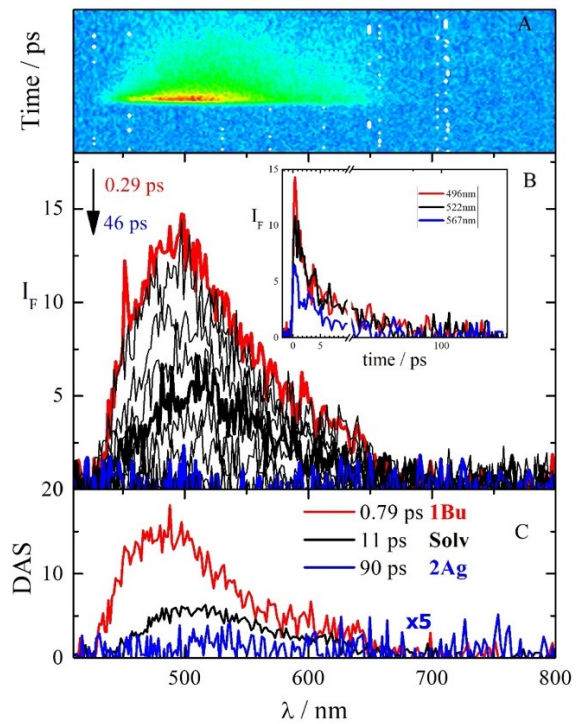


Figure ESI.13. Femtosecond Fluorescence Up-Conversion measurements of compound **DF** in Tol: experimental 3D data matrix (panel A); main time-resolved absorption spectra (panel B) and representative kinetics recorded at significant wavelengths (inset); Decay Associated Spectra (DAS) obtained by Global Analysis.

Table ESI.13. Femtosecond transient absorption and fluorescence up conversion measurements of compound DF in solvents of different polarizability.

Solvent	τ_{TA} / ps	τ_{FUC} / ps	Assignment
MeCH/3-MP	0.20 3.9 33 Inf		Solv. / B_u Solv. / VC A_g T_1
DHN	0.25 7.6 58 Inf		Solv. / B_u Solv. / VC A_g T_1
Tol ^a	0.86 9.2 89 Inf	0.79 11 90	Solv. / B_u Solv. / VC A_g T_1
Tol/An 9:1	0.57 7.5 49 Inf		Solv. / B_u Solv. / VC A_g (little ICT) T_1
Tol/An 7:3	0.49 7.1 64 Inf		Solv. / B_u Solv. / VC A_g mixed with ICT T_1
Tol/An 5:5 ^a	1.8 5.4 80 Inf		Solv. / B_u Solv. / VC A_g mixed with ICT T_1
An ^a	0.89 7.2 320 Inf		Solv. / B_u Solv. / VC ICT T_1
BrN	0.94 250 Inf		Solv. B_u T_1
DMSO ^a	0.46 2.8 84 1820 Inf		Solv. / B_u Solv. VC (ICT) ICT T_1

^a from ref. ⁷

Table ESI.14. Comparison between T_1 (green) and $2Ag$ (blue) ESA band as obtained by fs-TA experiments in the nanosecond and femtosecond regime for **2,5-(2TE)₂T** in solvents of different polarizability. $\Delta\lambda$ and ΔE relate to the T_1 spectral profile and $2Ag$ spectrum as obtained by fs-TA experiments.

Solvent	λ_{T_1} / nm (ns-TA)	λ_{T_1} / nm (fs-TA)	λ_{2Ag} /nm (fs-TA)	$\Delta\lambda$ /nm	ΔE / cm ⁻¹	ΔE / eV	Φ_T
Hx/PFHx	510	510	529	19	704	0.087	0.09
IP	510	513	533	20	731	0.091	0.09
DMSO	540	531	550	21	651	0.081	0.18
Tol	540	539	550	11	371	0.046	0.14
BrN	550	558	566	8	253	0.031	0.19

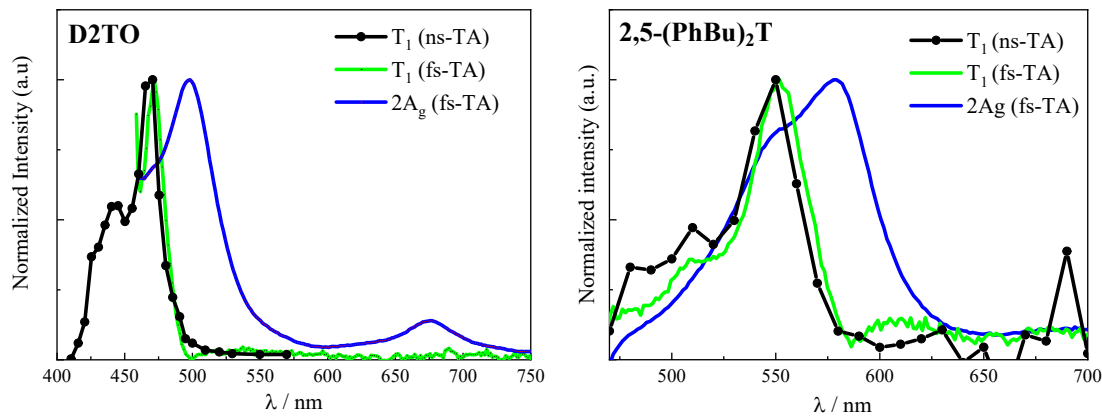


Figure ESI.14. Comparison between T_1 ESA spectra as obtained by ns-TA (black, scattered-line) and by fs-TA (green line) experiments and $2A_g$ ESA spectra as obtained by fs-TA experiments (blue) for compounds **D2TO** (left) and **2,5-(PhBu)₂T** (right) in Tol.

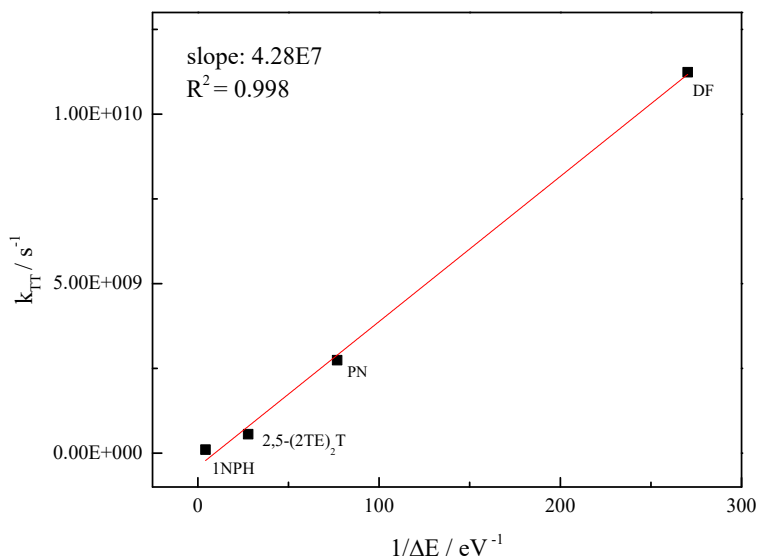


Figure ESI.15. Linear fitting of the $k_{TT}=1/\tau_{Ag}$ in function of the $1/\Delta E$, from the data reported in **Table 5** of the main paper. The ΔE are obtained from the difference between fs-TA ESA spectra of the $2Ag$ and T_1 states. The lifetimes of the Ag state are obtained from the fitting of fs-TA measurements.

5. Phosphorescence measurements

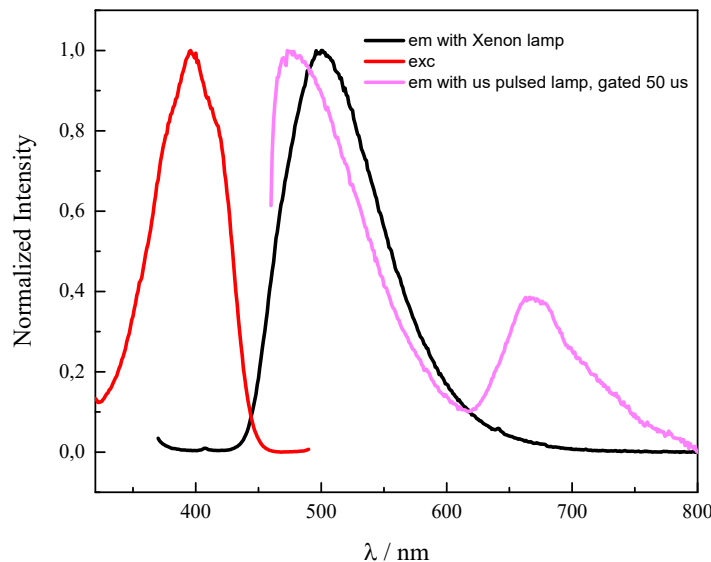


Figure ESI.16. Comparison between emission and excitation spectra of **DF** recorded at 77 K in MeCH-3MP matrix with different excitation sources.

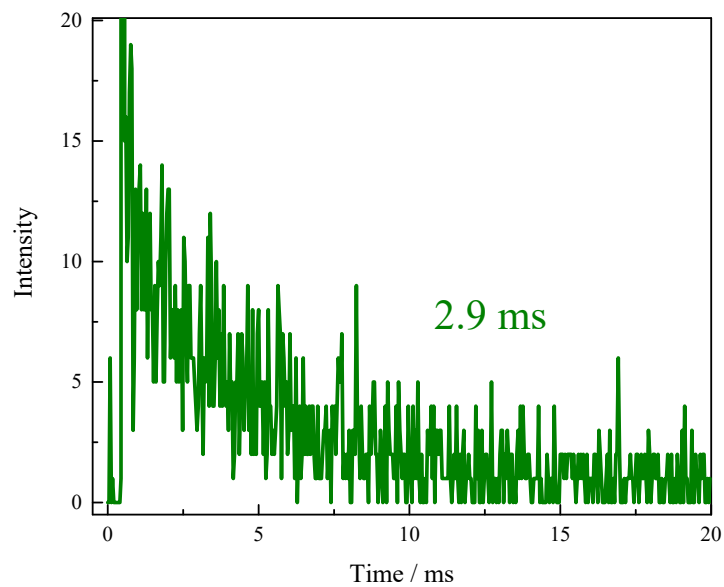


Figure ESI.17. Phosphorescence kinetic at 670 nm of **DF** recorded at 77 K in MeCH/3-MP matrix excited by 25 Hz pulsed lamp.

6. Quantum mechanical calculations

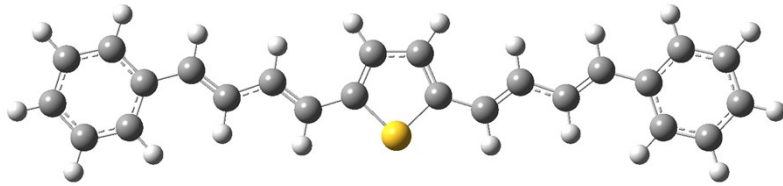


Figure ESI.18. Optimized S_0 geometry of compound **2,5-(PhBu)₂T**. Model: CAM-B3LYP/6-31+G(d,p) @ S_0 in cyclohexane.

Table ESI.15. Absorption and emission wavelengths (λ), oscillator strength (f) and molecular orbitals of **2,5-(PhBu)₂T** in cyclohexane (CPCM) calculated by the CAM-B3LYP/6-31+G(d,p)//CAM-B3LYP/6-31+G(d,p) model, together with the experimental absorption and emission maxima.

Transition	$\lambda_{\text{th}}/\text{nm}$	f	MO	%	$\lambda_{\text{exp}}/\text{nm}$
$S_0 \rightarrow T_1$	1016	0.0000	$\pi_H \rightarrow \pi_L^*$	86	
$S_0 \rightarrow T_2$	648	0.0000	$\pi_{H-1} \rightarrow \pi_L^*$	39	
			$\pi_H \rightarrow \pi_{L+1}^*$	46	
$S_0 \rightarrow T_3$	437	0.0000	$\pi_{H-2} \rightarrow \pi_L^*$	27	
			$\pi_{H-1} \rightarrow \pi_{L+1}^*$	24	
			$\pi_H \rightarrow \pi_{L+2}^*$	23	
$S_0 \rightarrow S_1$	425	2.7004	$\pi_H \rightarrow \pi_L^*$	92	420*
$S_0 \rightarrow T_4$	368	0.0000	$\pi_{H-2} \rightarrow \pi_{L+1}^*$	19	
			$\pi_H \rightarrow \pi_{L+10}^*$	21	
$S_0 \rightarrow T_5$	322	0.0000	$\pi_{H-7} \rightarrow \pi_L^*$	14	
			$\pi_{H-6} \rightarrow \pi_{L+1}^*$	11	
			$\pi_{H-4} \rightarrow \pi_{L+4}^*$	11	
			$\pi_{H-3} \rightarrow \pi_{L+3}^*$	15	
$S_0 \rightarrow S_2$	321	0.0042	$\pi_H \rightarrow \pi_{L+1}^*$	67	
$S_0 \rightarrow T_6$	312	0.0000	$\pi_{H-5} \rightarrow \pi_L^*$	49	
$S_0 \rightarrow T_7$	295	0.0000	$\pi_{H-5} \rightarrow \pi_L^*$	25	
$S_0 \rightarrow T_8$	290	0.0000	$\pi_{H-1} \rightarrow \pi_L^*$	15	
			$\pi_H \rightarrow \pi_{L+1}^*$	19	
			$\pi_H \rightarrow \pi_{L+3}^*$	15	
$S_0 \rightarrow T_9$	288	0.0000	$\pi_{H-1} \rightarrow \pi_{L+3}^*$	21	
			$\pi_H \rightarrow \pi_{L+4}^*$	18	
$S_0 \rightarrow T_{10}$	286	0.0000	$\pi_{H-4} \rightarrow \pi_{L+1}^*$	13	
			$\pi_{H-3} \rightarrow \pi_L^*$	13	
			$\pi_{H-1} \rightarrow \pi_{L+4}^*$	11	
			$\pi_H \rightarrow \pi_{L+1}^*$	11	
$S_0 \rightarrow S_3$	284	0.0019	$\pi_{H-1} \rightarrow \pi_L^*$	63	
$S_0 \rightarrow S_4$	264	0.2594	$\pi_H \rightarrow \pi_{L+2}^*$	47	

$S_0 \rightarrow S_5$	257	0.0060	$\pi_H \rightarrow \pi_{L+3}^*$	37	
$S_0 \rightarrow S_6$	254	0.1412	$\pi_{H-4} \rightarrow \pi_L^*$ $\pi_H \rightarrow \pi_{L+4}^*$	16 23	
$S_0 \rightarrow S_7$	253	0.0005	$\pi_H \rightarrow \pi_{L+6}^*$	60	
$S_0 \rightarrow S_8$	249	0.0896	$\pi_{H-5} \rightarrow \pi_L^*$	74	
$S_0 \rightarrow S_9$	244	0.0000	$\pi_H \rightarrow \pi_{L+5}^*$	74	
$S_0 \rightarrow S_{10}$	243	0.0186	$\pi_{H-2} \rightarrow \pi_L^*$ $\pi_H \rightarrow \pi_{L+2}^*$	38 30	
$S_1 \rightarrow S_0$	552	2.7326	$\pi_H \rightarrow \pi_L^*$	96	561*

*From the spectra recorded in MeCH/3-MP 9:1

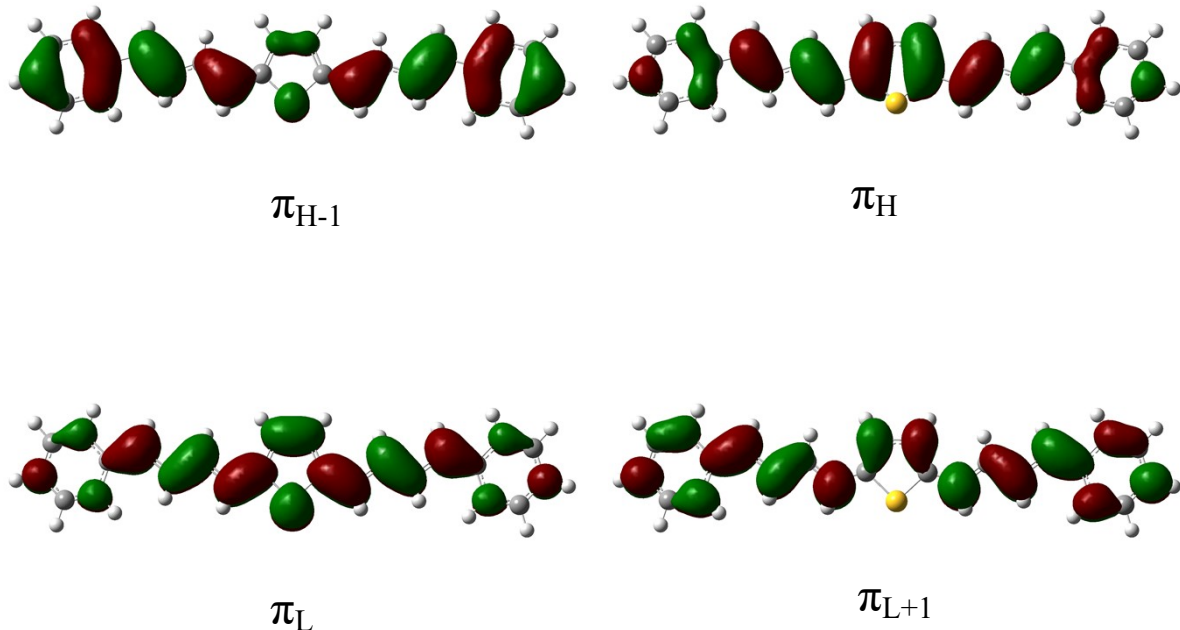


Figure ESI.19. Frontier molecular orbitals of **2,5-(PhBu)₂T**.

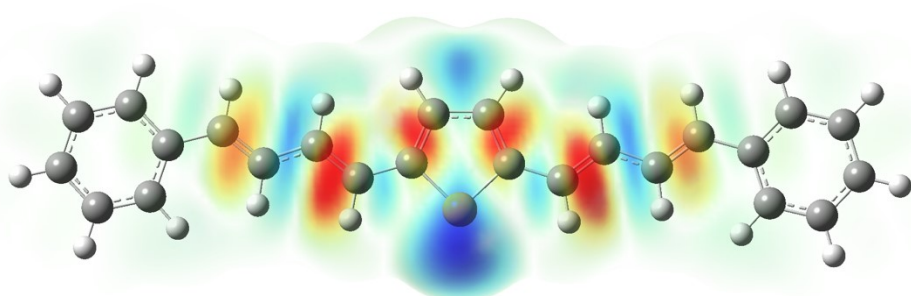


Figure ESI.20. Effect of the $S_0 \rightarrow S_1$ transition on the electron density of **2,5-(PhBu)₂T**; increase and decrease of electron densities are represented by blue (+0.00007) and red (-0.00007), respectively.

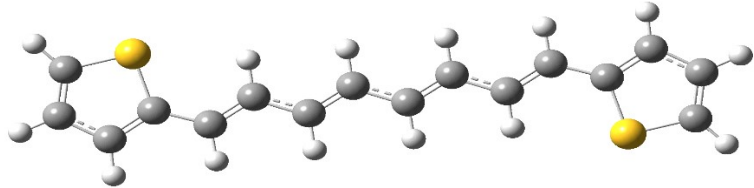


Figure ESI.21. Optimized S_0 geometry of compound **D2TO**. Model: CAM-B3LYP/6-31+G(d,p) @ S_0 in cyclohexane.

Table ESI.16. Absorption and emission wavelengths (λ), oscillator strength (f) and molecular orbitals of **D2TO** in cyclohexane (CPCM) calculated by the CAM-B3LYP/6-31+G(d,p)//CAM-B3LYP/6-31+G(d,p) model, together with the experimental absorption and emission maxima.

Transition	$\lambda_{\text{th}}/\text{nm}$	f	MO	%	$\lambda_{\text{exp}}/\text{nm}$
$S_0 \rightarrow T_1$	1196	0.0000	$\pi_H \rightarrow \pi_L^*$	99	
$S_0 \rightarrow T_2$	576	0.0000	$\pi_{H-1} \rightarrow \pi_L^*$	45	
			$\pi_H \rightarrow \pi_{L+1}^*$	43	
$S_0 \rightarrow T_3$	411	0.0000	$\pi_{H-4} \rightarrow \pi_L^*$	31	
			$\pi_{H-1} \rightarrow \pi_{L+1}^*$	28	
			$\pi_H \rightarrow \pi_{L+5}^*$	27	
$S_0 \rightarrow S_1$	410	2.5046	$\pi_H \rightarrow \pi_L^*$	94	396*
$S_0 \rightarrow T_4$	329	0.0000	$\pi_{H-5} \rightarrow \pi_L^*$	26	
$S_0 \rightarrow T_5$	301	0.0000	$\pi_{H-3} \rightarrow \pi_{L+1}^*$	34	
			$\pi_{H-2} \rightarrow \pi_L^*$	43	
$S_0 \rightarrow S_2$	301	0.0000	$\pi_{H-1} \rightarrow \pi_L^*$	46	
			$\pi_H \rightarrow \pi_{L+1}^*$	48	
$S_0 \rightarrow T_6$	301	0.0000	$\pi_{H-3} \rightarrow \pi_L^*$	48	
$S_0 \rightarrow T_7$	281	0.0000	$\pi_{H-1} \rightarrow \pi_L^*$	43	
			$\pi_H \rightarrow \pi_{L+1}^*$	45	
$S_0 \rightarrow T_8$	276	0.0000	$\pi_{H-6} \rightarrow \pi_L^*$	23	
$S_0 \rightarrow S_3$	275	0.0000	$\pi_{H-1} \rightarrow \pi_L^*$	46	
			$\pi_H \rightarrow \pi_{L+1}^*$	44	
$S_0 \rightarrow T_9$	250	0.0000	$\pi_H \rightarrow \pi_{L+12}^*$	28	
$S_0 \rightarrow T_{10}$	246	0.0000	$\pi_H \rightarrow \pi_{L+3}^*$	37	
			$\pi_H \rightarrow \pi_{L+4}^*$	47	
$S_0 \rightarrow S_4$	244	0.3104	$\pi_{H-2} \rightarrow \pi_L^*$	55	
$S_0 \rightarrow S_5$	244	0.0001	$\pi_H \rightarrow \pi_{L+4}^*$	54	
$S_0 \rightarrow S_6$	242	0.0000	$\pi_{H-3} \rightarrow \pi_L^*$	67	
$S_0 \rightarrow S_7$	241	0.0075	$\pi_H \rightarrow \pi_{L+6}^*$	44	
$S_0 \rightarrow S_8$	235	0.0000	$\pi_H \rightarrow \pi_{L+2}^*$	56	
$S_0 \rightarrow S_9$	230	0.0031	$\pi_H \rightarrow \pi_{L+3}^*$	36	
			$\pi_H \rightarrow \pi_{L+4}^*$	31	
$S_0 \rightarrow S_{10}$	230	0.0428	$\pi_{H-4} \rightarrow \pi_L^*$	60	
$S_1 \rightarrow S_0$	534	2.5856	$\pi_H \rightarrow \pi_L^*$	97	579*

*From the spectra recorded in MeCH/3-MP 9:1

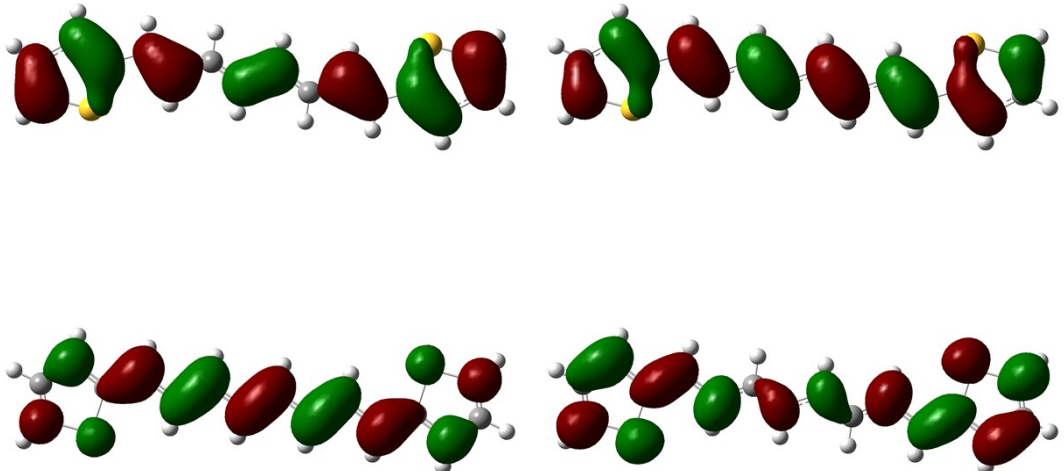


Figure ESI.22. Frontier molecular orbitals of **D2TO**.

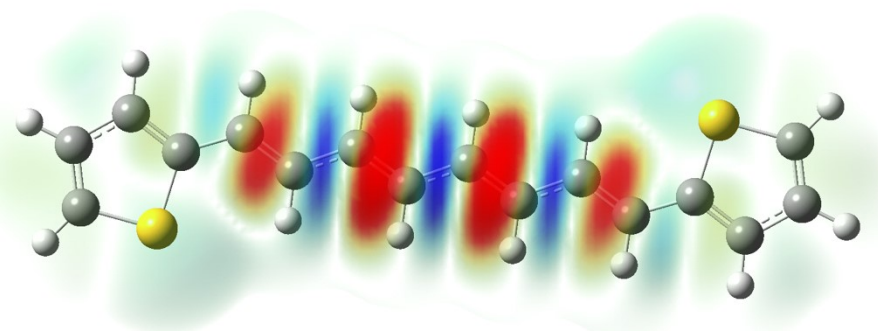


Figure ESI.23. Effect of the $S_0 \rightarrow S_1$ transition on the electron density of **D2TO**; increase and decrease of electron densities are represented by blue (+0.00008) and red (-0.00008), respectively.

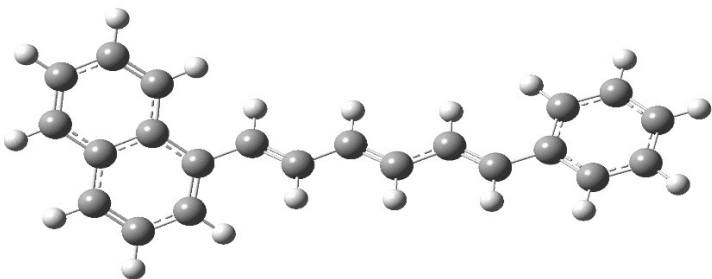


Figure ESI.24. Optimized S_0 geometry of compound **1NPH**. Model: CAM-B3LYP/6-31+G(d,p) @ S_0 in cyclohexane.

Table ESI.17. Absorption and emission wavelengths (λ), oscillator strength (f) and molecular orbitals of **1NPH** in cyclohexane (CPCM) calculated by the CAM-B3LYP/6-31+G(d,p)//CAM-B3LYP/6-31+G(d,p) model, together with the experimental absorption and emission maxima.

Transition	$\lambda_{\text{th}}/\text{nm}$	f	MO	%	$\lambda_{\text{exp}}/\text{nm}$
$S_0 \rightarrow T_1$	833	0.0000	$\pi_H \rightarrow \pi_L^*$	84	
$S_0 \rightarrow T_2$	509	0.0000	$\pi_{H-1} \rightarrow \pi_L^*$	34	
			$\pi_H \rightarrow \pi_{L+1}^*$	34	
$S_0 \rightarrow T_3$	400	0.0000	$\pi_{H-4} \rightarrow \pi_L^*$	25	
			$\pi_{H-1} \rightarrow \pi_{L+1}^*$	21	
$S_0 \rightarrow S_1$	366	2.0698	$\pi_H \rightarrow \pi_L^*$	94	359*
$S_0 \rightarrow T_4$	328	0.0000	$\pi_{H-5} \rightarrow \pi_L^*$	14	
			$\pi_{H-2} \rightarrow \pi_{L+3}^*$	13	
$S_0 \rightarrow T_5$	309	0.0000	$\pi_{H-2} \rightarrow \pi_L^*$	21	
			$\pi_{H-2} \rightarrow \pi_{L+1}^*$	22	
			$\pi_{H-1} \rightarrow \pi_{L+2}^*$	20	
			$\pi_H \rightarrow \pi_{L+2}^*$	21	
$S_0 \rightarrow T_6$	298	0.0000	$\pi_{H-3} \rightarrow \pi_{L+3}^*$	19	
$S_0 \rightarrow T_7$	292	0.0000	$\pi_{H-2} \rightarrow \pi_L^*$	23	
			$\pi_{H-2} \rightarrow \pi_{L+1}^*$	24	
			$\pi_{H-1} \rightarrow \pi_{L+2}^*$	21	
			$\pi_H \rightarrow \pi_{L+2}^*$	25	
$S_0 \rightarrow S_2$	288	0.0777	$\pi_{H-1} \rightarrow \pi_L^*$	40	
			$\pi_H \rightarrow \pi_{L+1}^*$	50	
$S_0 \rightarrow T_8$	287	0.0000	$\pi_{H-3} \rightarrow \pi_L^*$	19	
			$\pi_H \rightarrow \pi_{L+3}^*$	21	
$S_0 \rightarrow S_3$	277	0.0000	$\pi_{H-2} \rightarrow \pi_L^*$	25	
			$\pi_{H-2} \rightarrow \pi_{L+1}^*$	21	
			$\pi_{H-1} \rightarrow \pi_{L+2}^*$	21	
			$\pi_H \rightarrow \pi_{L+2}^*$	28	
$S_0 \rightarrow T_9$	275	0.0000	$\pi_{H-2} \rightarrow \pi_{L+2}^*$	79	
$S_0 \rightarrow T_{10}$	270	0.0000	$\pi_{H-4} \rightarrow \pi_{L+3}^*$	11	
			$\pi_{H-3} \rightarrow \pi_{L+3}^*$	11	
$S_0 \rightarrow S_4$	263	0.0014	$\pi_{H-1} \rightarrow \pi_L^*$	49	
			$\pi_H \rightarrow \pi_{L+1}^*$	38	
$S_0 \rightarrow S_5$	255	0.0112	$\pi_H \rightarrow \pi_{L+3}^*$	36	
$S_0 \rightarrow S_6$	243	0.0193	$\pi_{H-1} \rightarrow \pi_{L+1}^*$	35	

$S_0 \rightarrow S_7$	233	0.5411	$\pi_{H-2} \rightarrow \pi_L^*$ $\pi_H \rightarrow \pi_{L+2}^*$	25 32	
$S_0 \rightarrow S_8$	231	0.1412	$\pi_H \rightarrow \pi_{L+4}^*$ $\pi_H \rightarrow \pi_{L+5}^*$	18 20	
$S_0 \rightarrow S_9$	228	0.0222	$\pi_{H-4} \rightarrow \pi_L^*$	37	
$S_0 \rightarrow S_{10}$	226	0.0890	$\pi_H \rightarrow \pi_{L+5}^*$ $\pi_H \rightarrow \pi_{L+6}^*$	28 20	
$S_1 \rightarrow S_0$	496	2.1163	$\pi_H \rightarrow \pi_L^*$	97	472*

*From the spectra recorded in MeCH/3-MP 9:1

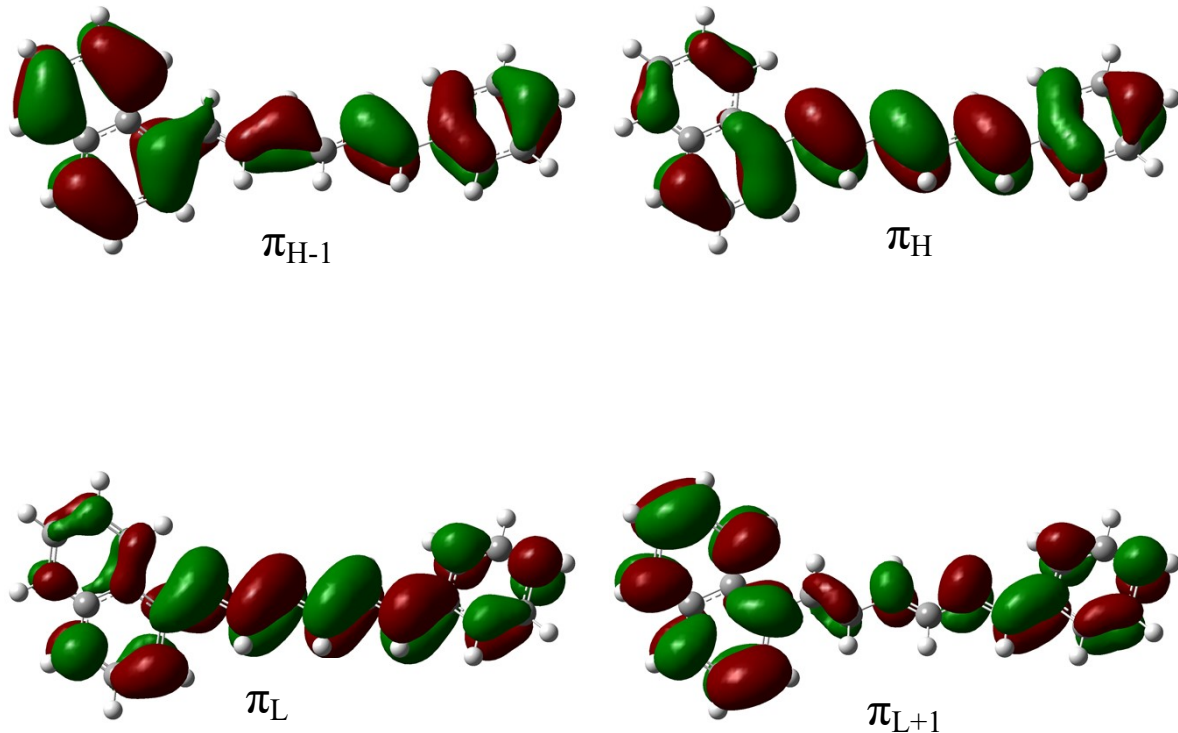


Figure ESI.25. Frontier molecular orbitals of **1NPH**.

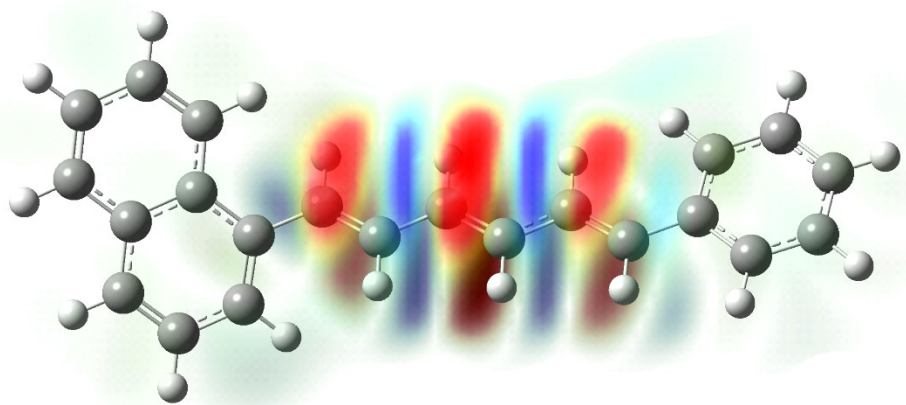


Figure ESI.26. Effect of the S₀→S₁ transition on the electron density of **1NPH**; increase and decrease of electron densities are represented by blue (+0.00008) and red (-0.00008), respectively.

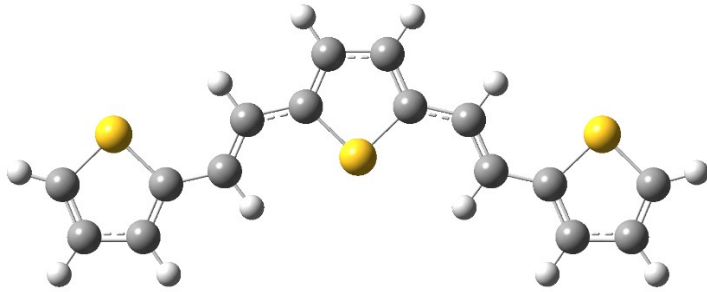


Figure ESI.27. Optimized S_0 geometry of compound **2,5-(2TE)₂T**. Model: CAM-B3LYP/6-31+G(d,p) @ S_0 in cyclohexane.

Table ESI.18. Absorption and emission wavelengths (λ), oscillator strength (f) and molecular orbitals of **2,5-(2TE)₂T** in cyclohexane (CPCM) calculated by the CAM-B3LYP/6-31+G(d,p)//CAM-B3LYP/6-31+G(d,p) model, together with the experimental absorption and emission maxima.

Transition	$\lambda_{\text{th}}/\text{nm}$	f	MO	%	$\lambda_{\text{exp}}/\text{nm}$
$S_0 \rightarrow T_1$	911	0.0000	$\pi_H \rightarrow \pi_L^*$	90	
$S_0 \rightarrow T_2$	559	0.0000	$\pi_{H-1} \rightarrow \pi_L^*$	42	
			$\pi_H \rightarrow \pi_{L+1}^*$	44	
$S_0 \rightarrow S_1$	413	1.4416	$\pi_H \rightarrow \pi_L^*$	94	413*
$S_0 \rightarrow T_3$	400	0.0000	$\pi_{H-5} \rightarrow \pi_L^*$	29	
			$\pi_{H-1} \rightarrow \pi_{L+1}^*$	27	
			$\pi_H \rightarrow \pi_{L+3}^*$	28	
$S_0 \rightarrow T_4$	322	0.0000	$\pi_{H-4} \rightarrow \pi_L^*$	23	
$S_0 \rightarrow T_5$	312	0.0000	$\pi_{H-4} \rightarrow \pi_L^*$	53	
$S_0 \rightarrow S_2$	304	0.2045	$\pi_{H-1} \rightarrow \pi_L^*$	45	
			$\pi_H \rightarrow \pi_{L+1}^*$	48	
$S_0 \rightarrow T_6$	301	0.0000	$\pi_{H-3} \rightarrow \pi_{L+1}^*$	33	
			$\pi_{H-2} \rightarrow \pi_L^*$	44	
$S_0 \rightarrow T_7$	300	0.0000	$\pi_{H-3} \rightarrow \pi_L^*$	46	
			$\pi_{H-2} \rightarrow \pi_{L+1}^*$	32	
$S_0 \rightarrow T_8$	279	0.0000	$\pi_{H-1} \rightarrow \pi_L^*$	42	
			$\pi_H \rightarrow \pi_{L+1}^*$	41	
$S_0 \rightarrow T_9$	273	0.0000	$\pi_{H-8} \rightarrow \pi_L^*$	22	
			$\pi_{H-6} \rightarrow \pi_{L+1}^*$	13	
			$\pi_{H-5} \rightarrow \pi_{L+3}^*$	12	
$S_0 \rightarrow S_3$	272	0.0000	$\pi_{H-1} \rightarrow \pi_L^*$	48	
			$\pi_H \rightarrow \pi_{L+1}^*$	42	
$S_0 \rightarrow S_4$	256	0.1028	$\pi_{H-4} \rightarrow \pi_L^*$	85	
$S_0 \rightarrow S_5$	251	0.0764	$\pi_H \rightarrow \pi_{L+3}^*$	52	
$S_0 \rightarrow T_{10}$	248	0.0000	$\pi_H \rightarrow \pi_{L+7}^*$	35	
$S_0 \rightarrow S_6$	243	0.0000	$\pi_H \rightarrow \pi_{L+2}^*$	73	
$S_0 \rightarrow S_7$	243	0.0140	$\pi_{H-2} \rightarrow \pi_L^*$	60	
$S_0 \rightarrow S_8$	242	0.2068	$\pi_{H-3} \rightarrow \pi_L^*$	65	
$S_0 \rightarrow S_9$	241	0.0011	$\pi_H \rightarrow \pi_{L+7}^*$	35	
$S_0 \rightarrow S_{10}$	230	0.0000	$\pi_H \rightarrow \pi_{L+5}^*$	50	

$S_1 \rightarrow S_0$	533	1.4613	$\pi_H \rightarrow \pi_L^*$	97	489*
-----------------------	-----	--------	-----------------------------	----	------

*From the spectra recorded in Tol

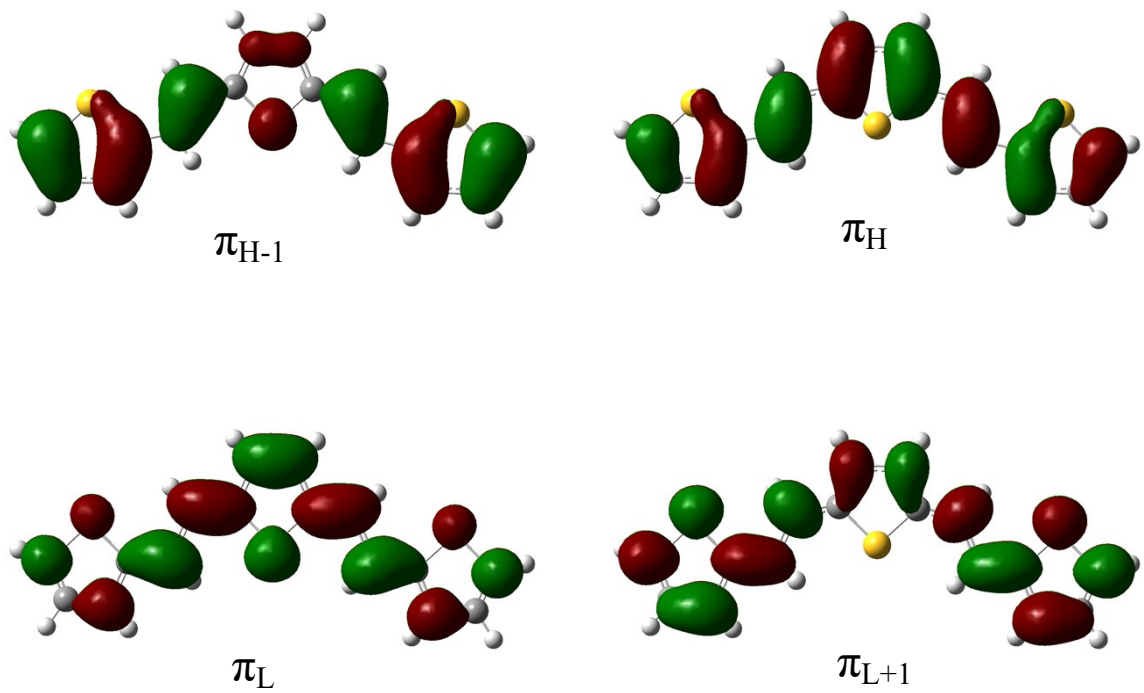


Figure ESI.28. Frontier molecular orbitals of **2,5-(2TE)₂T**.

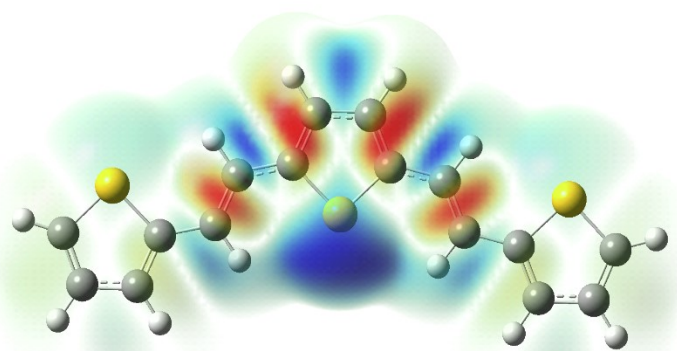
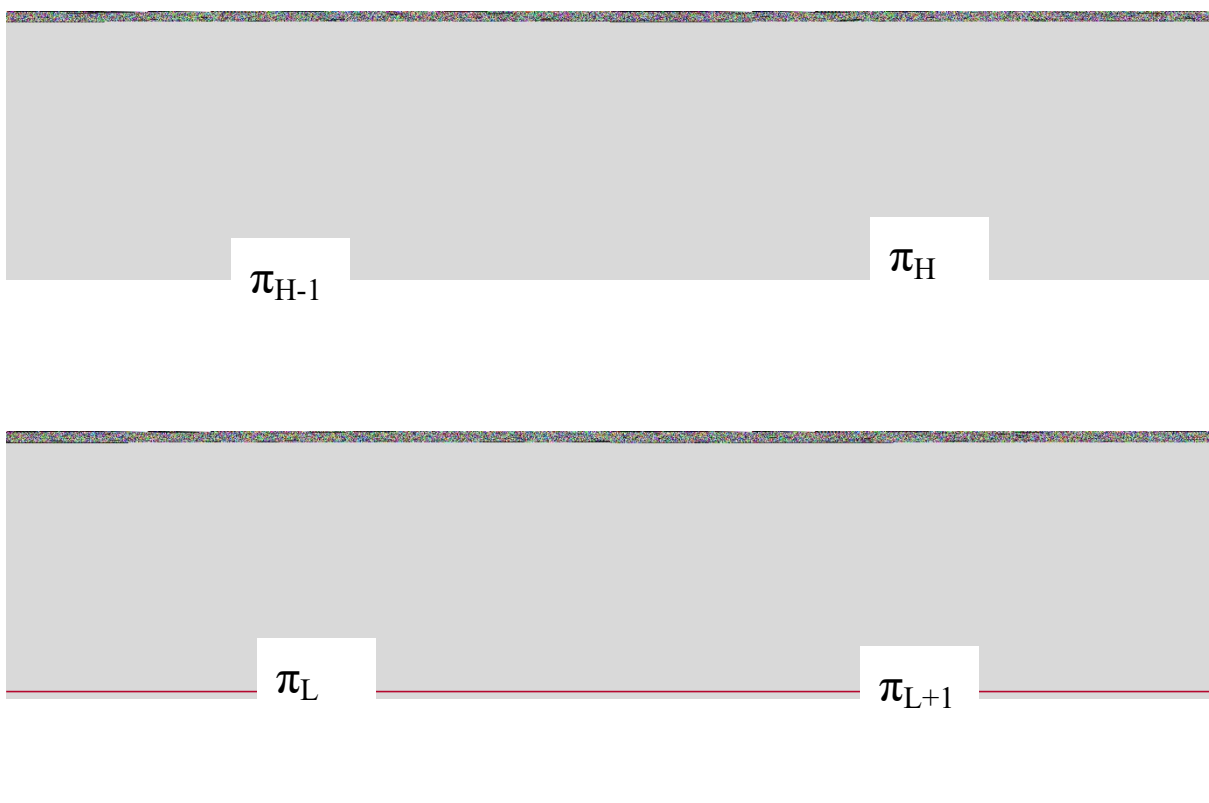


Figure ESI.29. Effect of the $S_0 \rightarrow S_1$ transition on the electron density of **2,5-(2TE)₂T**; increase and decrease of electron densities are represented by blue (+0.00008) and red (-0.00008), respectively.



The quantum mechanical calculations on **DF** have already been reported in a previous paper.⁷

- 1 B. Carlotti, A. Cesaretti, G. Cacioppa, F. Elisei, I. Odak, I. Škorić and A. Spalletti, *Journal of Photochemistry and Photobiology A: Chemistry*, 2019, **368**, 190–199.
- 2 E. Marri, G. Galiazzo and A. Spalletti, *Photochem Photobiol Sci*, 2004, **3**, 205–210.
- 3 G. Bartocci, A. Spalletti, R. S. Becker, F. Elisei, S. Floridi and U. Mazzucato, *J. Am. Chem. Soc.*, 1999, **121**, 1065–1075.
- 4 E. Marri, G. Galiazzo, F. Masetti, U. Mazzucato, C. Zuccaccia and A. Spalletti, *Journal of Photochemistry and Photobiology A: Chemistry*, 2005, **174**, 181–186.
- 5 M. Montalti, A. Credi, L. Prodi and M. T. Gandolfi, *Handbook of Photochemistry*, CRC Press, Boca Raton, 3rd edn., 2006.
- 6 I. Carmichael and G. L. Hug, *Journal of Physical and Chemical Reference Data*, 1986, **15**, 1–250.
- 7 L. Mencaroni, B. Carlotti, A. Cesaretti, F. Elisei, A. Grgičević, I. Škorić and A. Spalletti, *Photochem. Photobiol. Sci.*, 2020, **19**, 1665–1676.
- 8 G. Ginocchietti, G. Galiazzo, U. Mazzucato and A. Spalletti, *Photochem Photobiol Sci*, 2005, **4**, 547–553.
- 9 X. Allonas, C. Ley, C. Bibaut, P. Jacques and J. P. Fouassier, *Chemical Physics Letters*, 2000, **322**, 483–490.
- 10 A. Samanta, B. Ramachandram and G. Saroja, *Journal of Photochemistry and Photobiology A: Chemistry*, 1996, **101**, 29–32.
- 11 L. Mencaroni, B. Carlotti, F. Elisei, A. Marrocchi and A. Spalletti, *Chem. Sci.*, 2022, **13**, 2071–2078.
- 12 B. Carlotti, M. Poddar, F. Elisei, A. Spalletti and R. Misra, *J. Phys. Chem. C*, 2019, **123**, 24362–24374.
- 13 T. D. Giacco, B. Carlotti, S. De Solis, A. Barbaiana and F. Elisei, *Phys. Chem. Chem. Phys.*, 2010, **12**, 8062.
- 14 A. Mazzoli, A. Spalletti, B. Carlotti, C. Emiliani, C. G. Fortuna, L. Urbanelli, L. Tarpani and R. Germani, *J. Phys. Chem. B*, 2015, **119**, 1483–1495.

- 15 W. Dai, T. Bianconi, E. Ferraguzzi, X. Wu, Y. Lei, J. Shi, B. Tong, B. Carlotti, Z. Cai and Y. Dong, *ACS Materials Lett.*, 2021, 1767–1777.
- 16 M. J. Frisch, G. W. Trucks, H. B. Schlegel, G. E. Scuseria, M. A. Robb, J. R. Cheeseman, G. Scalmani, V. Barone, G. A. Petersson and H. Nakatsuji, .
- 17 S. Tortorella, M. M. Talamo, A. Cardone, M. Pastore and F. De Angelis, *J. Phys.: Condens. Matter*, 2016, **28**, 074005.
- 18 V. Barone and M. Cossi, *J. Phys. Chem. A*, 1998, **102**, 1995–2001.
- 19 B. Carlotti, F. Elisei, U. Mazzucato and A. Spalletti, *Phys. Chem. Chem. Phys.*, 2015, **17**, 14740–14749.